



Contents lists available at ScienceDirect

Inorganica Chimica Acta

journal homepage: www.elsevier.com/locate/ica

The synthesis, photophysical properties and water oxidation studies of a series of novel photosensitizer–catalyst assemblies

Neelima V. Nair^{*}, Rongwei Zhou, Randolph P. Thummel

Department of Chemistry, 3585 Cullen Blvd. Room 112, University of Houston, Houston, TX 77204-5003, United States

ARTICLE INFO

Article history:

Received 26 August 2015
Received in revised form 24 February 2016
Accepted 27 February 2016
Available online xxx

Keywords:

Asymmetric ditopic polypyridine bridging ligands
Ru(II) photosensitizer–catalyst assemblies
Energy and electron transfer
Electrocatalytic water oxidation

ABSTRACT

A novel series of bridging ligands and their Ru^{II} photosensitizer–catalyst dyads have been prepared and characterized by NMR and electronic absorption spectroscopy as well as cyclic voltammetry. The presence of asymmetry in the ligands facilitated selective metal coordination, which greatly enhanced the ease of the preparation of the dyads. The photophysical properties of the photosensitizers and the photosensitizer–catalyst dyads were also studied. All the photosensitizers were found to be strong emitters while the extremely weak emission of the dyads suggested quenching by either energy or electron transfer. The water oxidation activities of the dyads have been evaluated under both light and Ce^{IV} activated conditions. The dyads were found to be active under Ce^{IV} activated conditions. Electrochemical studies also suggest that these systems may be used as electrocatalysts for photoelectrochemical water oxidation.

© 2016 Elsevier B.V. All rights reserved.

1. Introduction

In recent years, a growing interest in the direct conversion of solar energy into environment-friendly fuels has led to intensified research in the area of artificial photosynthesis [1]. Tremendous efforts are being made to develop light-driven water splitting systems that evolve molecular hydrogen and oxygen. A practical, cost-effective technology capable of catalytically splitting water into its elements using sunlight has not yet been achieved. Research involving homogeneous catalysis of water splitting has led to systems evolving either hydrogen or oxygen, but not both in the same system. Since water oxidation as a half-reaction is considered to be the energy demanding bottleneck as far as the construction of such devices is concerned, the development of efficient light-driven water oxidation systems is highly desirable.

Recently, our group reported the photosensitizer–water oxidation catalyst dyad **1** [2], and the groups of Meyer and Sun reported systems **2** [3] and **3** [4], respectively (Fig. 1). Systems **1** and **3** were found to generate oxygen more efficiently than the respective systems composed of separate photosensitizer and water oxidation catalyst, while **2** exhibited activity similar to its corresponding 3-component system.

The aforementioned enhancement in activity of **1** and **3** was attributed to the fact that, covalent linking allowed for

intramolecular electron transfer between the photosensitizer and catalyst moieties, whereas in the systems composed of separate photosensitizer and water oxidation catalyst, electron transfer would be intermolecular.

We reasoned that moving the metal centers within a water oxidation dyad farther apart would perhaps retard the back-electron transfer to the catalyst which can lower the efficiency of a dyad. For this reason, we began to explore possibilities for constructing dyads in which the metal centers are separated by para-phenylene linkers. However, initial studies showed that the synthesis of a dyad from a symmetric bridging ligand is extremely difficult, owing to the poor selectivity between the binding sites during complexation. After much consideration, we realized that the selectivity between binding sites in a bridging ligand could be improved by introducing asymmetry within the molecule. Thus, a series of ligands was prepared using Sonogashira and Suzuki coupling reactions (Fig. 2, ligands **4–8**).

The first ligand prepared in this series was **7**. The complexation of **7** with [Ru(bpy)₂Cl₂] in a 1:1 fashion provided only the desired mononuclear complex, allowing us to proceed further by incorporating the catalyst in the tridentate site. Having overcome the difficulties previously encountered in the synthesis of a dyad, we were encouraged to prepare the remaining ligands in the series and their corresponding chromophore–catalyst assemblies.

^{*} Corresponding author.

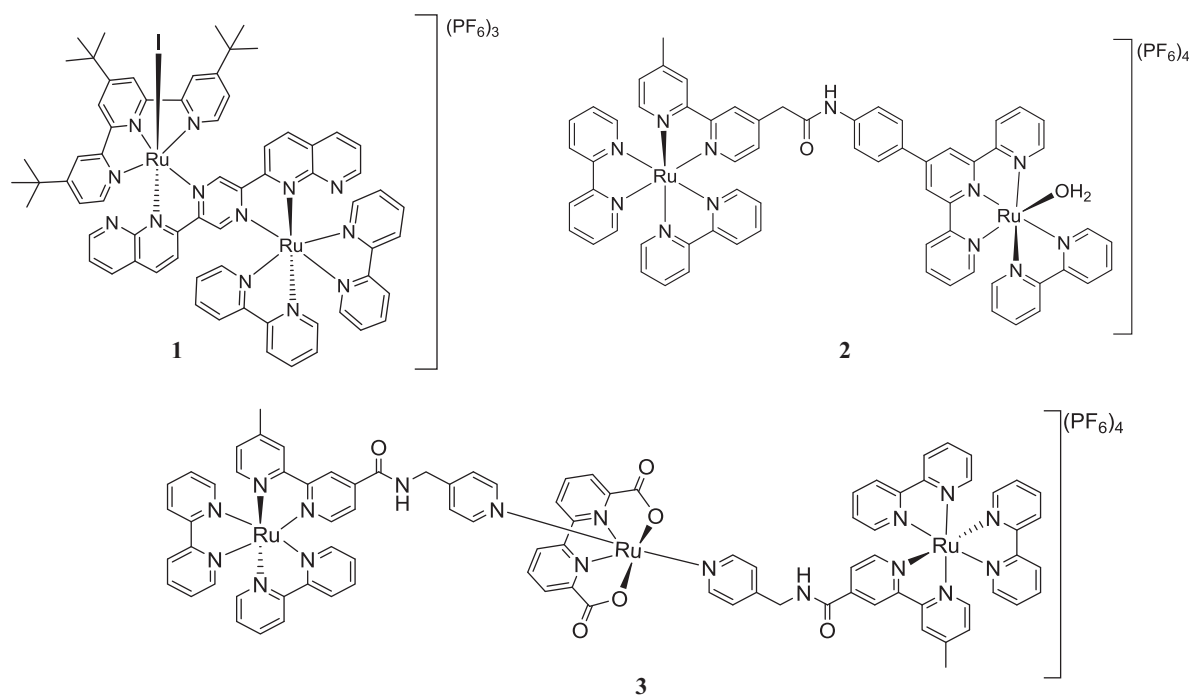


Fig. 1. Structures of photosensitizer–catalyst assemblies **1**, **2** and **3**.

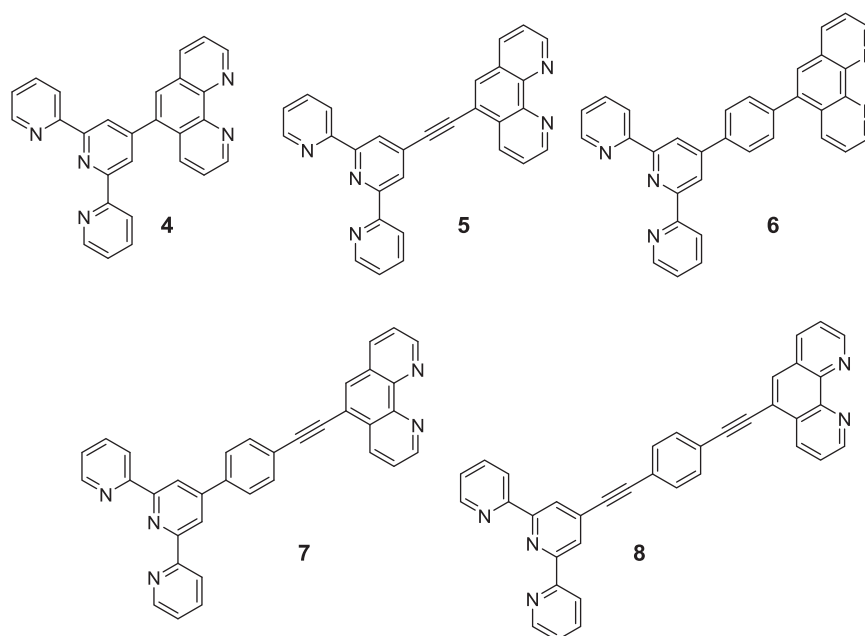


Fig. 2. Structures of bridging ligands **4–8**.

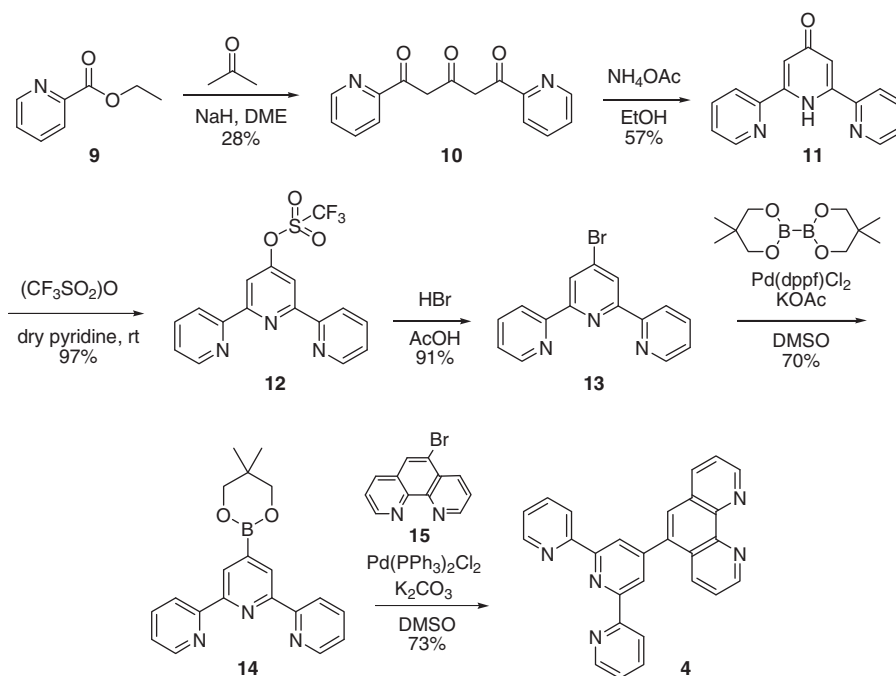
2. Results and discussion

2.1. Synthesis and characterization

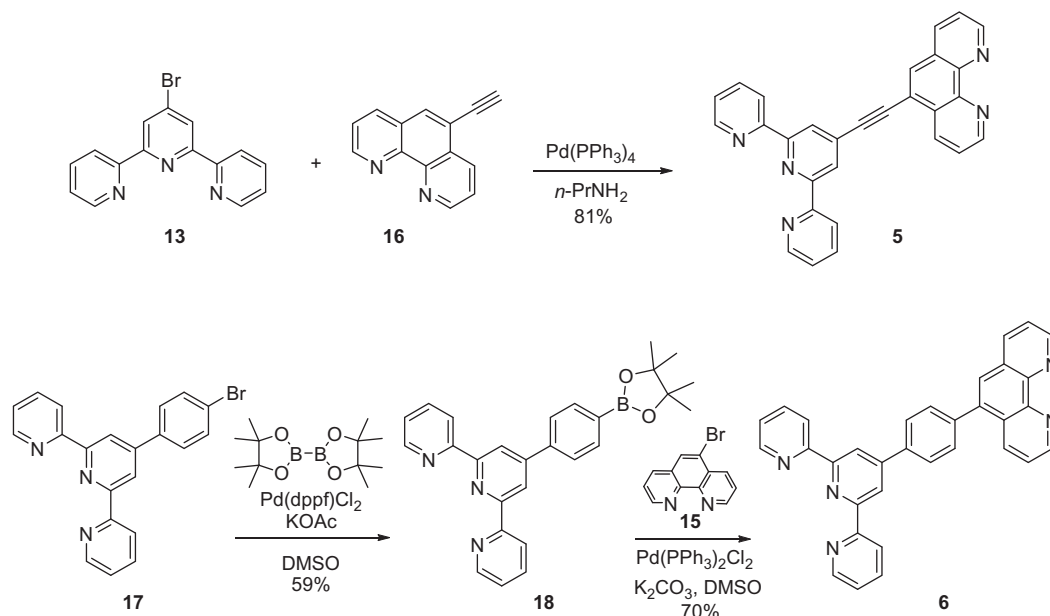
Ligand **4** was synthesized in 6 steps (Scheme 1), starting from the commercially available 2-ethylpicolinate (**9**), which was condensed with acetone in the presence of NaH to provide 1,5-bis(2'-pyridyl)pentane-1,3,5-trione (**10**) in 28% yield. Compound **10** was then subjected to a Kröhnke reaction using NH_4OAc to obtain **11** (57%), which was then treated with triflic anhydride to afford compound **12** in 97% yield. The bromination of **12** was then carried

out to obtain 4'-bromo-2,2':6',2''-terpyridine (**13**) in 91% yield, following which a Miyaura borylation using bis(neopentyl glycolato) diboron (B_2neo_2) provided the terpyridine boronate ester **14** (70%). A Suzuki coupling reaction between **14** and 5-bromo-1,10-phenanthroline, **15**, prepared according to a previously reported method [5], was then carried out to provide ligand **4** (73%).

A Sonogashira coupling reaction between 5-ethynyl-1,10-phenanthroline, **16**, prepared using the procedure reported by Ziesel et al. [6], and 4'-bromo-2,2':6',2''-terpyridine (**13**) provided ligand **5** in 81% yield. In order to prepare ligand **6**, 4'-(4-bromophenyl)-2,2':6',2''-terpyridine (**17**, prepared according to a



Scheme 1. Synthesis of ligand 4.



Scheme 2. Syntheses of ligands 5 and 6.

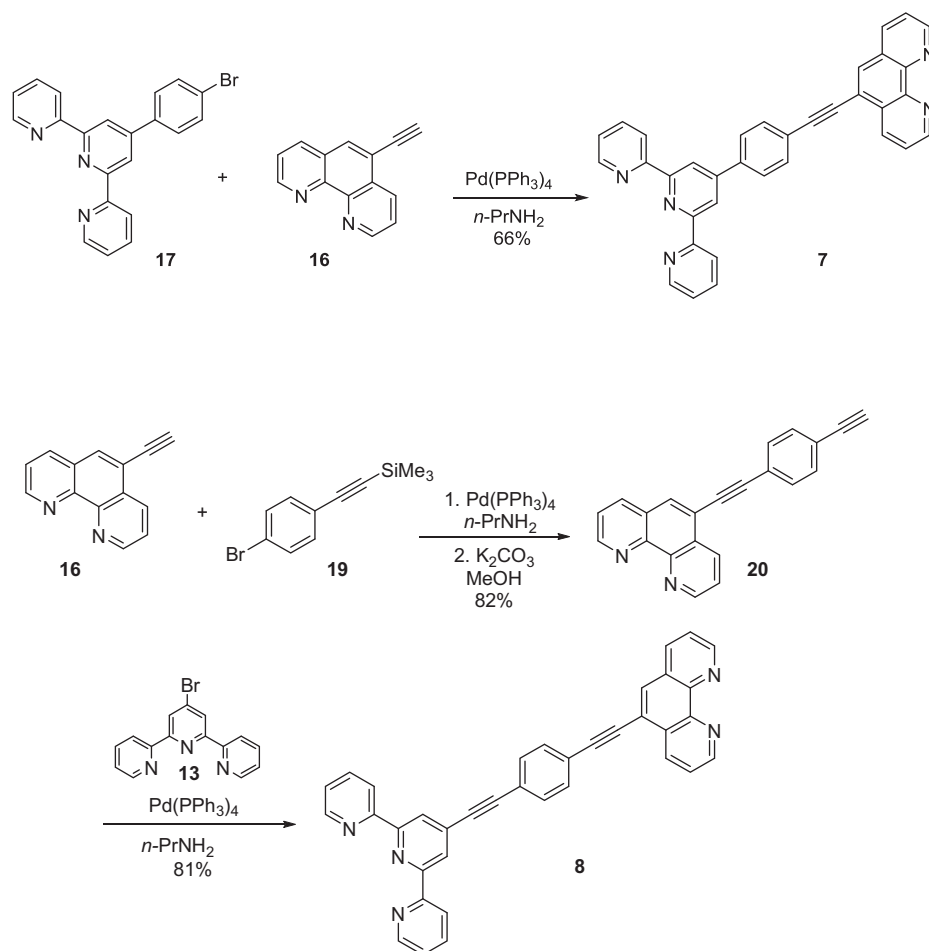
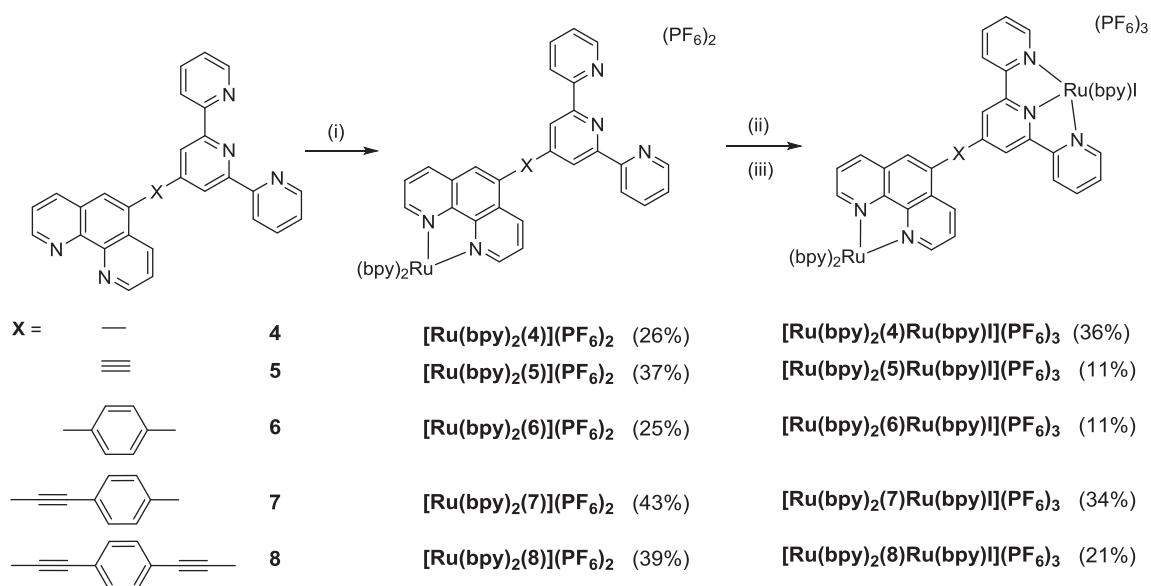
reported method [7]) was borylated using bis(pinacolato)diboron (B_2pin_2) to obtain the boronate ester **18** (59%). A Suzuki reaction between **18** and **15** was then carried out, affording ligand **6** in 70% yield (Scheme 2).

A Sonogashira coupling reaction between **16** and **17** was carried out to provide ligand **7** in 66% yield. The synthesis of ligand **8** was accomplished in 2 steps: a Sonogashira reaction between **16** and the commercially available **19**, followed by deprotection of the silyl group provided the compound **20** in 82% yield. Further reaction of **20** with **13** afforded ligand **8** in 81% yield (Scheme 3).

Ligands **4–8** were used to prepare their corresponding chromophore–catalyst assemblies in 3 steps, according to the general

procedure outlined in Scheme 4. In the first step, each ligand was reacted with $[Ru(bpy)_2Cl_2]$ in a 1:1 fashion to insert the sensitizer portion into the bidentate site. Subsequently, each sensitizer was reacted with $[Ru(bpy)(dmsO)_2Cl_2]$ to provide the dyads as chloride complexes. Each chloride complex was then treated with KI to provide the corresponding iodo-complex.

The bridging ligands (BLs), photosensitizers and dyads were characterized primarily by 1H NMR spectroscopy. Proton inventories, characteristic splitting patterns and H–H COSY NMR were used to assign the protons of the ligands. The 1H NMR spectra of **4** and **6** are shown below (Fig. 3). In these systems, the signals for H2 and H9 of the phenanthroline moiety were found to overlap

Scheme 3. Syntheses of ligands **7** and **8**.Scheme 4. Syntheses of photosensitizers and dyads **4–8**. (i) $[\text{Ru}(\text{bpy})_2\text{Cl}_2]$, EtOH–H₂O (3:1) reflux, then aq. NH₄PF₆ (ii) $[\text{Ru}(\text{bpy})(\text{dmsO})_2\text{Cl}_2]$, EtOH reflux, then aq. NH₄PF₆ (iii) KI, acetone/H₂O (1:1) reflux, then aq. NH₄PF₆; % yields are shown in parentheses.

at ca. 9.3 and 9.2 ppm respectively. The H14 doublet in **4** overlapped with the 2H-singlet for H10 at ca. 8.7 ppm. The H4 and H7 protons of the phenanthroline portion appeared very close

together near 8.4 ppm, but could be distinguished. The signal for H6 of phenanthroline appeared as a singlet at ca. 8.2 ppm. The H12 proton present in the terpyridine portion produced a triplet

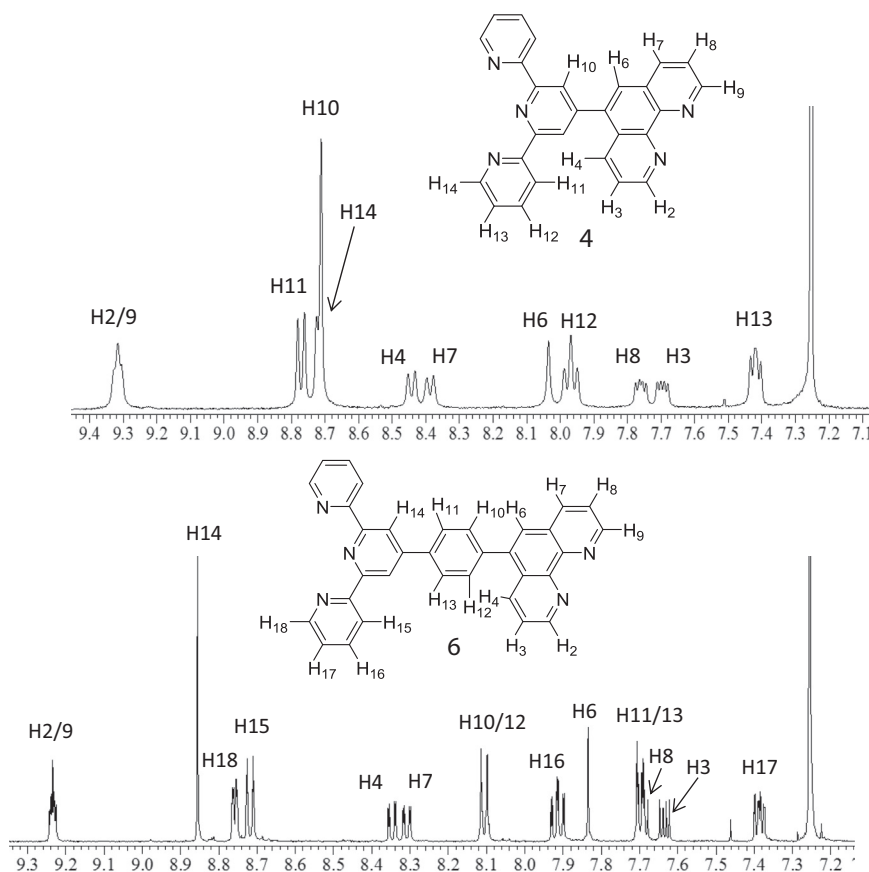


Fig. 3. ^1H NMR spectra of **4** and **6** in CDCl_3 with proton assignments.

of doublets at *ca.* 8.0 ppm, as is commonly seen for this proton. In the spectrum of **6**, the singlet corresponding to the terpyridyl proton H14 was shifted downfield by *ca.* 2.5 ppm relative to its counterpart, H10, in **4**. Thus the doublet for H18 could be distinguished unlike its counterpart in **4**. A pair of doublets belonging to the central phenyl ring in **6** was observed at 8.1 and 7.7 ppm. The H8 proton from the phenanthroline moiety was found to overlap with the phenyl proton doublet at 7.7 ppm. Similar observations were made in the case of **5**, **7** and **8** (Fig. 4).

In the spectrum of **5** (Fig. 4), all the signals were clearly visible without any overlaps. The H6 of the phenanthroline portion was shifted downfield relative to **4** due to the deshielding effect of the ethynyl group. The signals for the phenyl ring protons in **8** were shifted closer together (<1 ppm apart) compared to **7** (~2 ppm apart) and **5** (~4 ppm apart), probably because in **8**, both sets of protons (H10/H12 and H11/H13) are in a similar environment, being flanked by ethynyl groups on either side.

The length of the linkers in each of the bridging ligands was estimated using DFT calculations. The Ru–Ru distances in the corresponding dyads of ligands **4–8** were estimated in our laboratory using molecular modelling and were found to be 12.89, 15.81, 17.47, 19.81 and 22.24 Å, respectively. The nature of the linker is expected to have an influence on intramolecular electron transfer, and hence, communication between the two metal centers. Thus, by varying the linker, one can expect differences in the rates of electron transfer, which in turn influences the activity of these systems towards water oxidation (Fig. 5).

Electrochemistry was employed to characterize all the photosensitizers and dyads. The cyclic voltammograms of the sensitizers and dyads are shown in Figs. 6 and 7 and the redox data are summarized in Table 1. As shown in Fig. 6, all the sensitizers exhibited

a reversible redox couple near 1.30 V versus Ag/AgCl, which was assigned to the $\text{Ru}^{\text{III/II}}$ couple. The potentials are similar to that of $[\text{Ru}(\text{bpy})_3]^{2+}$ (1.26 V), suggesting that ligand modification on a remote position has little impact on the electronics of the Ru^{II} center. All half-wave oxidation potentials seen in Fig. 6 were assigned to the photosensitizer $\text{Ru}_{\text{ps}}^{\text{III/II}}$. The anodic scan afforded ligand-based reduction couples. The first reductions of all the sensitizers occurred more positively compared to $[\text{Ru}(\text{bpy})_3]^{2+}$ (–1.33 V) or $[\text{Ru}(\text{phen})_3]^{2+}$ (–1.36 V). This shift helped in identifying the reduction waves as those of the bridging ligand. In all cases, there is a spike on the reductive site corresponding to the adsorption of neutral species generated after two one-electron processes at the electrode. The electrochemistry of the sensitizers suggests a Ru-based highest occupied molecular orbital (HOMO) and BL-based lowest occupied molecular orbital (LUMO).

A careful examination of the reductive chemistry of the sensitizers suggested a correlation between the first reduction and the nature of the bridging ligand. An anodic shift of *ca.* 80 mV was observed when an ethynyl group was inserted between the phen and tpy rings from the comparison between $[\text{Ru}(\text{bpy})_2(\mathbf{4})](\text{PF}_6)_2$ and $[\text{Ru}(\text{bpy})_2(\mathbf{5})](\text{PF}_6)_2$. This shift was attributed to the strong electron-withdrawing effect of the ethynyl group.

The coupling of a Ru^{II} catalyst moiety to the photosensitizers resulted in a redox couple around 0.80 V versus Ag/AgCl in all the dyads (Fig. 7). This oxidation potential, assigned to $\text{Ru}_{\text{cat}}^{\text{III/II}}$, was found to be similar to that of $[\text{Ru}(\text{tpy})(\text{bpy})\text{I}]^+$ (0.86 V), even in $[\text{Ru}(\text{bpy})_2(\mathbf{4})\text{Ru}(\text{bpy})\text{I}](\text{PF}_6)_3$ where the linker is short. The potentials of the $\text{Ru}_{\text{ps}}^{\text{III/II}}$ couple in all the dyads (1.29–1.34 V) were also identical to the corresponding sensitizers, suggesting no electronic communication between Ru_{ps} center and Ru_{cat} center in the ground state. In $[\text{Ru}(\text{bpy})_2(\mathbf{4})\text{Ru}(\text{bpy})\text{I}](\text{PF}_6)_3$, the phen and tpy

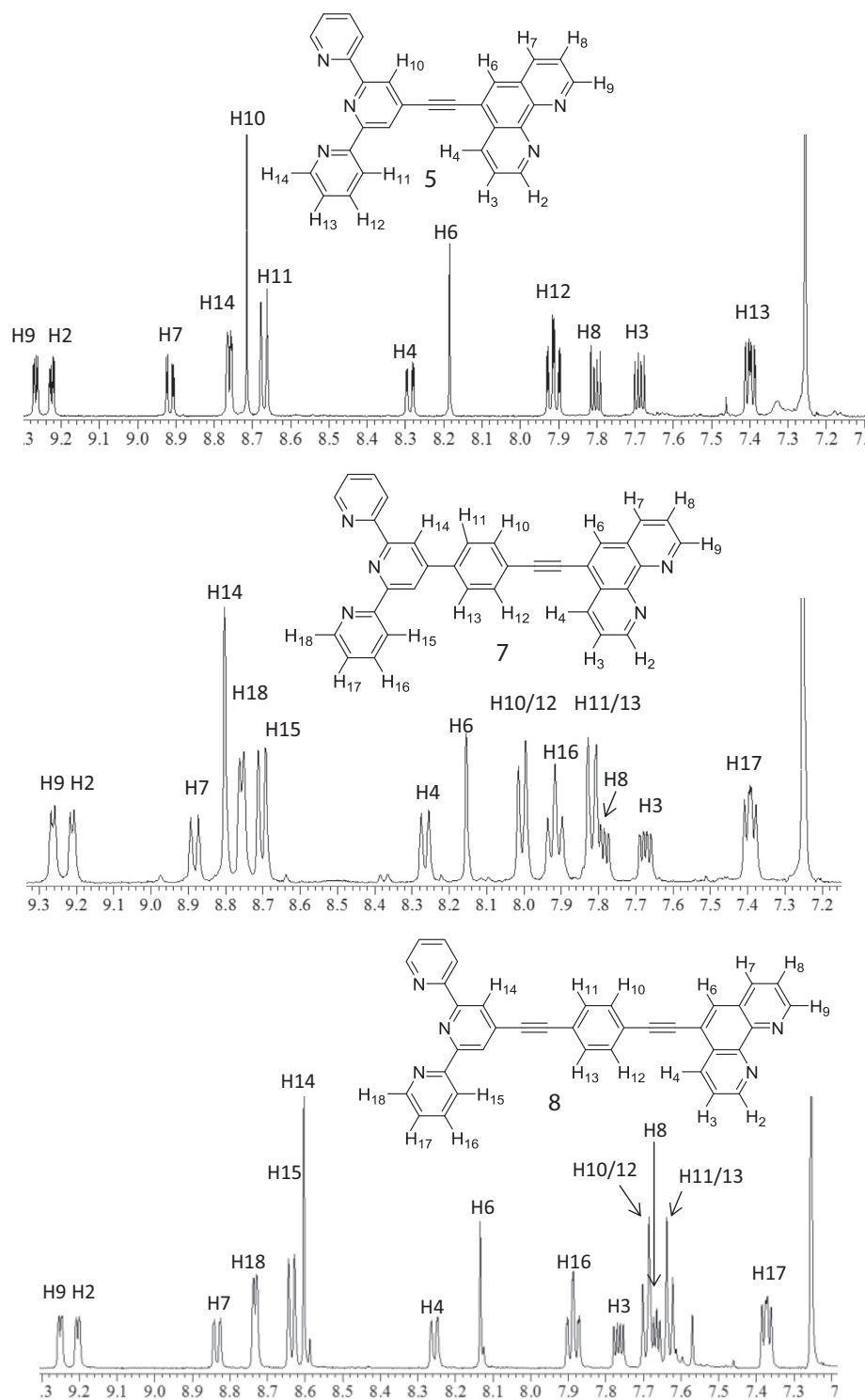


Fig. 4. ^1H NMR spectra of **5**, **7** and **8** in CDCl_3 with proton assignments.

rings are not coplanar due to steric effects, resulting in poor electronic communication between the two Ru centers. In other cases, although phen and tpy can be coplanar, the distance created by the linker between the two Ru centers could weaken the electronic communication. The fact that Ru_{cat} is more prone to be oxidized than the Ru_{ps} center suggests that Ru_{cat} can serve as electron donor to reduce the excited state of Ru_{ps} or $\text{Ru}_{\text{ps}}^{\text{III}}$ generated photochemically. The reduction waves of the dyads displayed a positive shift relative to the corresponding sensitizers due to the electron-with-

drawing nature of $[\text{Ru}(\text{tpy})(\text{bpy})\text{I}]^+$ unit. The CVs of the dyads suggest two HOMOs: $\text{Ru}_{\text{cat}}(d\pi)$ – based at higher energy and $\text{Ru}_{\text{ps}}(d\pi)$ – based at lower energy.

The electronic absorption spectra of the complexes were recorded in acetonitrile at room temperature (Fig. 8) and the data have been summarized in Table 1. The region from 250–400 nm was mainly attributed to the ligand $\pi \rightarrow \pi^*$ transitions. The presence of ethynyl and/or phenylene groups led to more conjugation and caused a red shift in the $\pi \rightarrow \pi^*$ transitions. As a result, going from

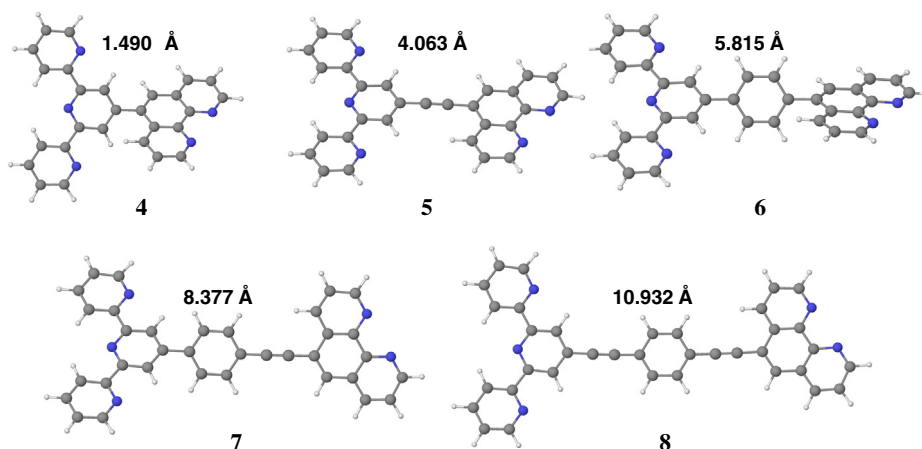


Fig. 5. Optimized structures of the ligands showing the length in Å of each linker.

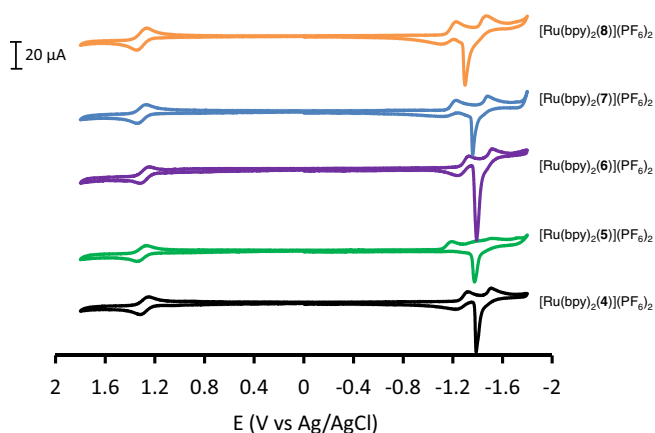


Fig. 6. Cyclic voltammograms of the sensitizers: 0.1 M Bu_4NPF_6 in CH_3CN , glassy carbon working electrode, Ag/AgCl reference electrode, and Pt auxiliary electrode; scan rate 100 mV/s.

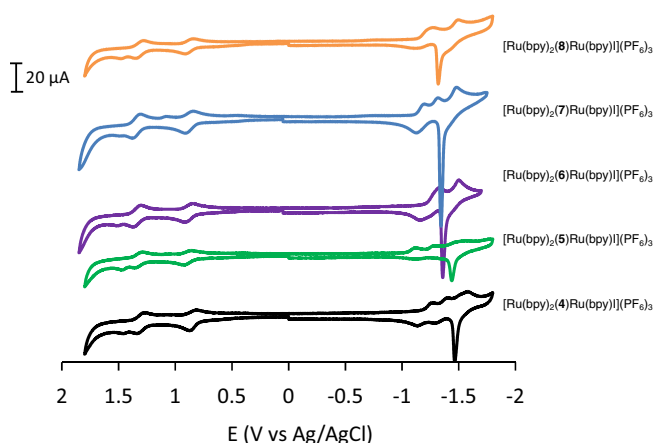


Fig. 7. Cyclic voltammograms of the dyads: conditions same as in Fig. 6.

$[\text{Ru}(\text{bpy})_2(\mathbf{4})](\text{PF}_6)_2$ to $[\text{Ru}(\text{bpy})_2(\mathbf{8})](\text{PF}_6)_2$, a higher intensity absorbance band developed around 350 nm, with the exception of $[\text{Ru}(\text{bpy})_2(\mathbf{6})](\text{PF}_6)_2$ which, interestingly, showed a spectrum similar to $[\text{Ru}(\text{bpy})_2(\mathbf{4})](\text{PF}_6)_2$. Similar behavior was observed in the dyads as well. The region from 400 to 600 nm was assigned

to the metal to ligand charge transfer (MLCT) transitions. The visible region in the spectra of the sensitizers is mainly $\text{Ru}(\text{d}\pi) \rightarrow \text{BL}(\pi^*)$ CT in character (Table 2).

As expected, the absorption spectra of the dyads showed two bands in the MLCT region. The bands at ca. 450 nm which were assigned to $\text{Ru}_{\text{ps}}(\text{d}\pi) \rightarrow \text{BL}(\pi^*)$ CT remained similar to the bands observed in the photosensitizers. However, subtle differences were observed in the bands at ca. 520 nm which were assigned to the $\text{Ru}_{\text{cat}}(\text{d}\pi) \rightarrow \text{BL}(\pi^*)$ CT, i.e. these bands were shifted to different extents depending on the nature of the bridging ligand. In $[\text{Ru}(\text{bpy})_2(\mathbf{4})\text{Ru}(\text{bpy})\text{I}](\text{PF}_6)_3$, the $\text{Ru}_{\text{cat}}(\text{d}\pi) \rightarrow \text{BL}(\pi^*)$ CT band was observed at 520 nm, while the corresponding band in $[\text{Ru}(\text{bpy})_2(\mathbf{8})\text{Ru}(\text{bpy})\text{I}](\text{PF}_6)_3$ was red-shifted to 530 nm. The presence of an ethynyl group clearly creates a red shift due to its strong electron-withdrawing effect; going from $[\text{Ru}(\text{bpy})_2(\mathbf{4})\text{Ru}(\text{bpy})\text{I}](\text{PF}_6)_3$ to $[\text{Ru}(\text{bpy})_2(\mathbf{5})\text{Ru}(\text{bpy})\text{I}](\text{PF}_6)_3$, a red shift of 520–538 nm was observed.

2.2. Photophysical Studies

Emission and excitation studies were carried out on the sensitizers and dyads using degassed acetonitrile solutions. The photosensitizers were found to be strong emitters, showing emission bands centered at 600 nm, with a quantum yield similar to that of $\text{Ru}(\text{bpy})_3^{2+}$ at ca. 0.065 (Fig. 9). The dyads were found to show extremely weak emission relative to the sensitizers. This observation suggests either energy transfer (from sensitizer to catalyst) or electron transfer (from catalyst to sensitizer) leading to the quenching of emission. The emission of the sensitizers was quenched by O_2 and therefore solutions which had not been degassed were found to exhibit lower emission intensity.

As shown in Fig. 9, all dyads displayed a weak emission around 750 nm and 600 nm when excited at 450 nm. The weak emission at 600 nm is attributed to Ru-chromophore emission. It is known that $[\text{Ru}(\text{tpy})(\text{bpy})\text{I}](\text{PF}_6)_3$ can emit weakly around 700 nm. Therefore the 750 nm emission band is attributed to ${}^3\text{Ru}_{\text{cat}}(\text{d}\pi) \rightarrow \text{TL}(\pi^*)$ CT (TL = terminal ligand). A red shift of this emission band in the dyads was observed, probably due to the perturbation of the bridging ligand π^* energy. In $[\text{Ru}(\text{bpy})_2(\mathbf{5})\text{Ru}(\text{bpy})\text{I}](\text{PF}_6)_3$ and $[\text{Ru}(\text{bpy})_2(\mathbf{8})\text{Ru}(\text{bpy})\text{I}](\text{PF}_6)_3$ the emission band was red-shifted to lower energy (~ 780 nm) due to the decrease of the ${}^3\text{Ru}_{\text{cat}}(\text{d}\pi) \rightarrow \text{TL}(\pi^*)$ CT energy. Interestingly, the emission bands from ${}^3\text{Ru}_{\text{cat}}(\text{d}\pi) \rightarrow \text{TL}(\pi^*)$ CT in the dyads are stronger than that of $[\text{Ru}(\text{tpy})(\text{bpy})\text{I}](\text{PF}_6)_3$ under the same conditions (emission spectrum included in Supporting information). In $[\text{Ru}(\text{tpy})(\text{bpy})\text{I}](\text{PF}_6)_3$, one quenching process is the thermal population of a

Table 1
Summary of electronic absorption^a, emission^b and cyclic voltammetric data^c for all complexes.

Compound	λ_{\max} (nm) (ϵ M ⁻¹ cm ⁻¹)	E_{em} (eV)	$E_{1/2}^{\text{ox}}$ (ΔE) (V)	$E_{1/2}^{\text{red}}$ (ΔE) (V)
[Ru(bpy) ₂ (4)](PF ₆) ₂	450 (16,800)	2.07	1.29 (80)	-1.25 (irr), -1.42 (irr), -1.58 (irr)
[Ru(bpy) ₂ (4)Ru(bpy)](PF ₆) ₃	453 (21,000), 520 (sh)	1.65	1.30 (60), 0.84 (50)	-1.29 (irr), -1.42 (irr), -1.58 (irr)
[Ru(bpy) ₂ (5)](PF ₆) ₂	451 (16,000)	2.07	1.32 (70)	-1.17 (irr), -1.50 (irr)
[Ru(bpy) ₂ (5)Ru(bpy)](PF ₆) ₃	451 (20,000), 538 (sh)	1.60	1.32 (50), 0.88 (50)	-1.10 (irr), -1.26 (irr)
[Ru(bpy) ₂ (6)](PF ₆) ₂	451 (17,000)	2.07	1.29 (80)	-1.28 (60), -1.51 (irr)
[Ru(bpy) ₂ (6)Ru(bpy)](PF ₆) ₃	454 (18,000), 516 (sh)	1.65	1.33 (60), 0.88 (50)	-1.31 (89), -1.51 (irr)
[Ru(bpy) ₂ (7)](PF ₆) ₂	451 (16,000)	2.07	1.32 (80)	-1.16 (90), -1.47 (irr)
[Ru(bpy) ₂ (7)Ru(bpy)](PF ₆) ₃	453 (26,000), 538 (sh)	1.63	1.34 (50), 0.86 (50)	-1.17 (55), -1.35 (irr), -1.47 (irr)
[Ru(bpy) ₂ (8)](PF ₆) ₂	451 (20,000)	2.07	1.32 (90)	-1.17 (90), -1.46 (irr)
[Ru(bpy) ₂ (8)Ru(bpy)](PF ₆) ₃	451 (25,000), 530 (sh)	1.60	1.31 (50), 0.88 (50)	-1.21 (80), -1.51 (irr)

^a Measured in CH₃CN at rt with sample concentration of 12 μ M.

^b Recorded in CH₃CN at rt; excitation at 450 nm.

^c Measured with a glassy carbon electrode at 100 mV/s in CH₃CN containing 0.1 M N(n-Bu)₄PF₆ and reported in volts relative to Ag/AgCl electrode.

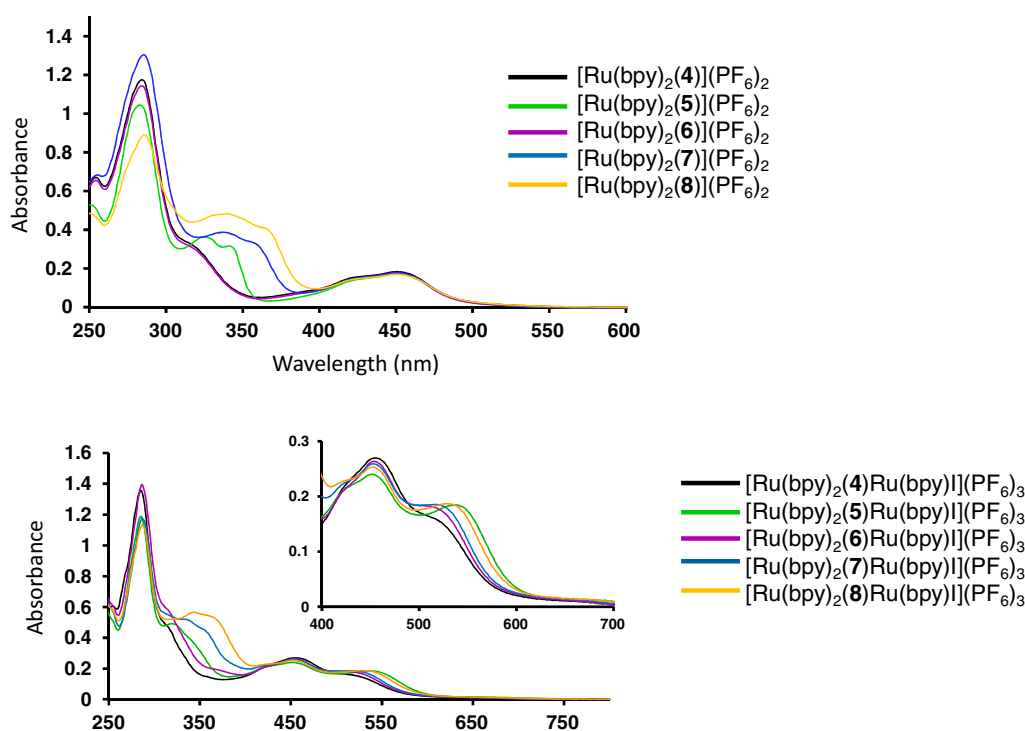


Fig. 8. Electronic absorption spectra of sensitizers (top) and dyads (bottom; inset shows MLCT bands) in CH₃CN at rt.

Table 2
Emission data of the dyads.^a

Compound	λ_{em} (nm)
[Ru(bpy) ₂ (4)Ru(bpy)](PF ₆) ₃	750
[Ru(bpy) ₂ (5)Ru(bpy)](PF ₆) ₃	780
[Ru(bpy) ₂ (6)Ru(bpy)](PF ₆) ₃	750
[Ru(bpy) ₂ (7)Ru(bpy)](PF ₆) ₃	760
[Ru(bpy) ₂ (8)Ru(bpy)](PF ₆) ₃	780
[Ru(tpy)(bpy)](PF ₆)	710

^a Recorded in CH₃CN at rt with excitation at 450 nm.

non-emissive, slightly higher energy $^3\pi \rightarrow \pi^*$ (tpy) excited state [8]. It is suggested that this $^3\pi \rightarrow \pi^*$ (tpy) orbital is raised higher in the dyads, thus impeding the quenching process, leading to higher emission intensity compared to [Ru(tpy)(bpy)](PF₆).

Excitation spectroscopy was used to monitor the 3 MLCT emission at 600 nm. The excitation spectra of the photosensitizers were found to be almost identical to the electronic absorption spectrum.

This led us to conclude that the 600 nm emission band arises from Ru(π) \rightarrow BL(π^*) CT observed in the absorbance spectrum. The excitation spectra of the dyads monitoring the 750 nm emission band, however, afforded excitation spectra different from the corresponding electronic absorption spectra. As seen in Fig. 10, the excitation spectrum of [Ru(bpy)₂(**4**)Ru(bpy)](PF₆)₃ exhibits a shoulder at ca. 450 nm and a band at 550 nm. This observation indicates that some portion of absorption band at ca. 450 nm, which is from chromophore 3 Ru_{ps}($d\pi$) \rightarrow BL(π^*) CT, contributes to catalyst-moiety 3 Ru_{ps}($d\pi$) \rightarrow BL(π^*) CT emission via energy transfer (Fig. 10).

The energy transfer from chromophore to catalyst-moiety is thermodynamically favorable as shown in the simplified energy state diagram for [Ru(bpy)₂(**4**)Ru(bpy)](PF₆)₃, where the energy of 1 MLCT was estimated from the redox potentials and absorption spectra and 3 MLCT energy was estimated from the excitation and emission spectra (Fig. 11).

It must be noted that the excitation spectrum of each dyad for the emission around 750 nm does not superimpose its absorption

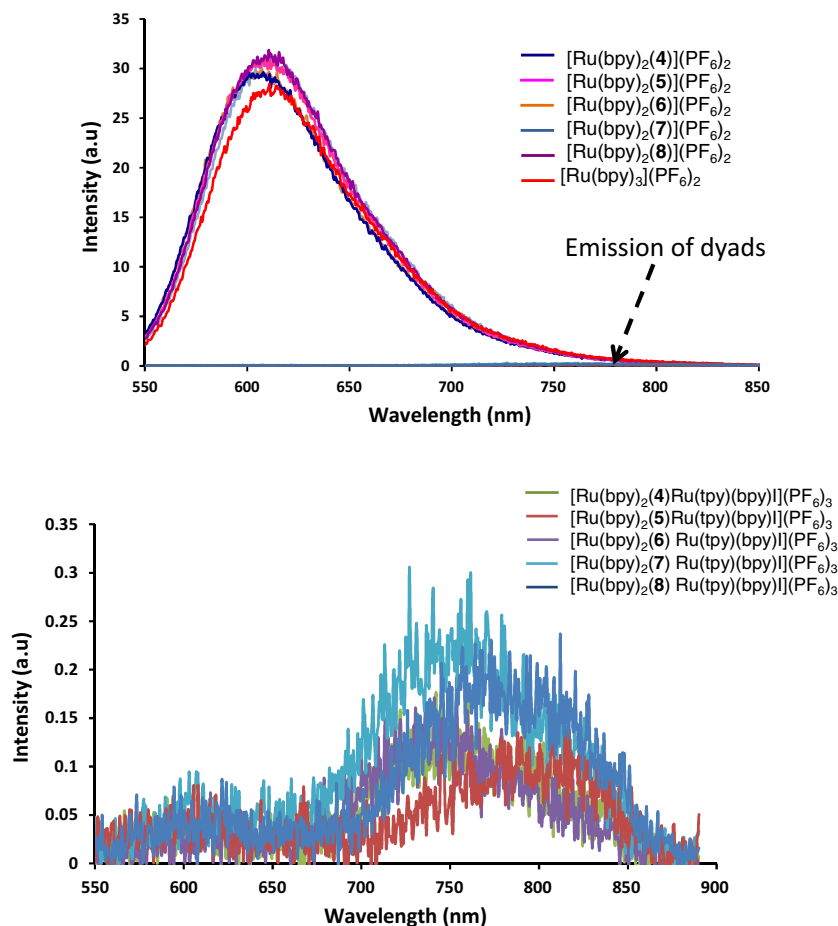


Fig. 9. Emission of photosensitizers, $\text{Ru}(\text{bpy})_3^{2+}$ and dyads in degassed CH_3CN at rt (top) and emission of dyads magnified (bottom).

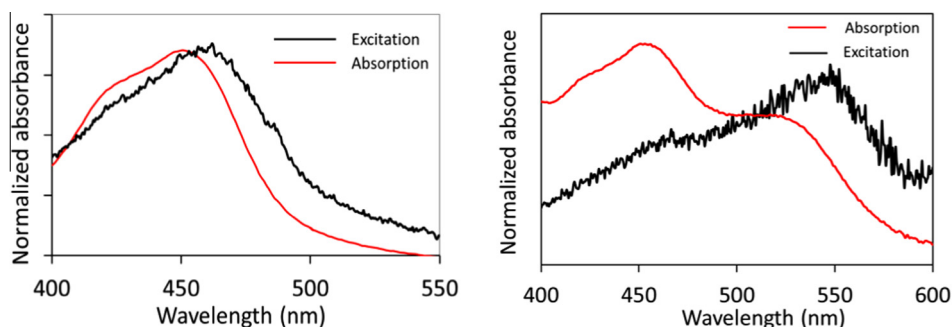


Fig. 10. Excitation spectra of $[\text{Ru}(\text{bpy})_2(4)](\text{PF}_6)_2$ (left) and dyad $[\text{Ru}(\text{bpy})_2(4)\text{Ru}(\text{tpy})(\text{bpy})](\text{PF}_6)_3$ (right) in CH_3CN monitoring the emission at 600 nm and 750 nm respectively.

spectrum. This indicates that energy transfer alone is not responsible for the quenching. Electron transfer possibly occurs based on electrochemical studies. From the CVs, the $\text{Ru}_{\text{cat}}^{\text{II/III}}$ oxidation is more negative than $\text{Ru}_{\text{ps}}^{\text{II/III}}$, which suggests that Ru_{cat} can be an electron donor to reductively quench the Ru_{ps} . The result of these two processes is the formation of Ru_{cat} with high oxidation state.

We also conducted a control experiment to demonstrate the efficiency of the quenching processes. We found that the emission of a solution containing 1 eq. each of $[\text{Ru}(\text{bpy})_2(5)](\text{PF}_6)_2$ and $[\text{Ru}(\text{tpy})(\text{bpy})](\text{PF}_6)$ is much higher than that of a solution containing $[\text{Ru}(\text{bpy})_2(5)\text{Ru}(\text{bpy})](\text{PF}_6)_3$ at the same concentration (Fig. 12). This suggests that intramolecular energy/electron transfer is much more efficient than the corresponding intermolecular process.

2.3. Water oxidation studies

The observed electron transfer and energy transfer processes between the chromophore and catalyst moieties encouraged us to test the photocatalytic water oxidation activity of the dyads. Following previously reported conditions [2], we tested the photocatalytic activities of all the dyads in $\text{Na}_2\text{SiF}_6/\text{NaHCO}_3$ buffer solution (pH 6) using $\text{Na}_2\text{S}_2\text{O}_8$ as electron acceptor and blue light (470 nm). However, the dyads did not produce any detectable O_2 . It is possible that although Ru_{cat} can be oxidized to Ru^{III} state, achieving higher valent ruthenium species for water oxidation did not take place due to the high thermodynamic driving force and possible back electron transfer. The addition of a large excess of

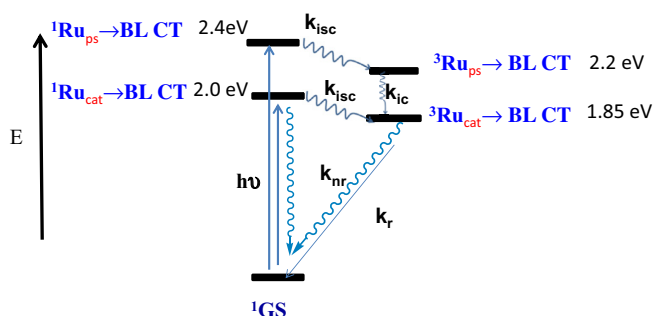


Fig. 11. Simplified energy state diagram depicting the photophysical properties of dyad $[\text{Ru}(\text{bpy})_2(4)\text{Ru}(\text{bpy})\text{I}](\text{PF}_6)_3$. The rate constants k_{isc} , k_{ic} , k_{nr} and k_r refer to intersystem crossing, internal conversion, non-radiative decay and radiative decay, respectively.

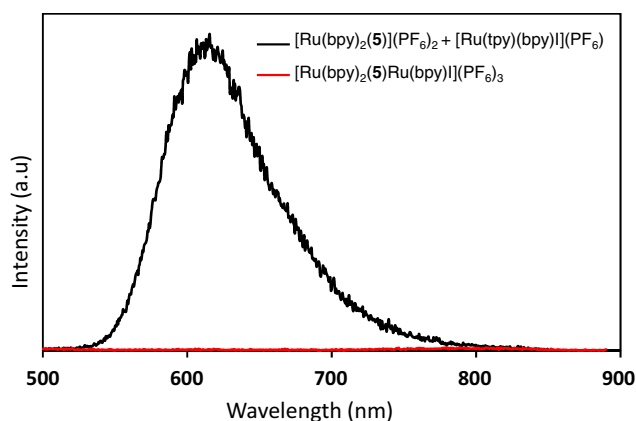


Fig. 12. Emission spectra of $[\text{bpy}]_2\text{Ru}(5)\text{Ru}(\text{bpy})\text{I}(\text{PF}_6)_3$ and a 1:1 mixture of $[\text{Ru}(\text{tpy})(\text{bpy})\text{I}]^+$ and $[(\text{bpy})_2\text{Ru}(5)]^{2+}$ in CH_3CN at rt. Excitation wavelength: 450 nm; concentration: 2.3 μM .

$[\text{Ru}(\text{bpy})_3]^{2+}$ (~100 eq.) resulted in the formation of a very small amount of O_2 (TON ~3 in 1 h). Attempts to modify the sensitizer component by replacing $\text{Ru}(\text{bpy})_2^-$ with $\text{Ru}(\text{Br}_2\text{phen})_2^-$ (Br_2phen = 5,6-dibromo-1,10-phenanthroline) to increase the oxidation potential of the sensitizer portion also did not improve the activity of these systems. Experiments carried out using Ce^{IV} , however, resulted in O_2 evolution from water, suggesting that the catalytic activity of Ru_{cat} is preserved. However, a regular trend was not observed and therefore the mechanism cannot be explained.

Electrochemical studies of the dyads in aqueous solution (pH 7) showed the development of a catalytic current (Fig. 13). The onset of catalytic current was observed at ca. 1.4 V in all cases. Based on this onset potential, the overpotential was estimated to be 600 mV for all the dyads. The fact that the dyads show electrocatalytic behavior and exhibit energy/electron transfer when irradiated with visible light suggest that they can potentially be used as catalysts for photoelectrochemical water oxidation.

3. Conclusions

A series of novel chromophore–catalyst dyads containing different linkers has been synthesized. The bridging ligands were prepared using Suzuki or Sonogashira reactions. The presence of asymmetry in the ligands facilitated selective metal coordination, which greatly enhanced the ease of the preparation of the dyads. The photosensitizers and dyads were characterized using ^1H NMR and electronic absorption spectroscopy as well as cyclic voltammetry. The photophysical properties of both the sensitizers and dyads have been studied. All the photosensitizers were found to be strong emitters, while the extremely weak emission of the

dyads suggested quenching by either energy or electron transfer. The analysis of excitation spectra suggest that the photosensitizers are capable of energy transfer, however, this may not be the main mode of quenching in the dyad. Electron transfer is probably the favored mode of quenching.

The lack of activity of these systems towards homogenous photocatalytic water oxidation is probably due to the high thermodynamic driving force, i.e. the excited state reduction potential of $[\text{Ru}(\text{bpy})_3]^{2+}$ (0.77 V) is not sufficiently high to drive water oxidation in these systems, as the oxidation potential of the catalyst portion is ca. 0.8 V [2]. The fact that these systems generate O_2 chemically suggests that the activity of the catalyst portion is retained in the dyads. Electrochemical analysis in aqueous pH 7 solution showed the development of catalytic current for all of the dyads. Therefore, these systems may be used as catalysts for photoelectrochemical water oxidation. Future studies will involve the modification of these systems to enable their immobilization on electrodes or nanoparticles such as TiO_2 or ZrO_2 by incorporating carboxyl groups in the sensitizer portion.

4. Experimental

4.1. Materials and methods

Compounds **10** [9], **11** [9], **12** [10], **13** [11], **14** [12], **15** [5], **16** [6], **17** [7], **18** [12], $[\text{Ru}(\text{bpy})(\text{dms})_2\text{Cl}_2]$ [13] and $[\text{Ru}(\text{bpy})_2\text{Cl}_2]$ [14] were prepared according to published procedures. All Suzuki [15] and Sonogashira [16] reactions were carried out according to the methods reported by Higuchi and Ziesel, respectively. Compound **19** was purchased from Sigma Aldrich; bis(pinacolato)diboron (B_2pin_2) and bis(neopentyl glycolato)diboron (B_2neo_2) were obtained from Oakwood Chemicals. DMSO was dried over 3 Å molecular sieves for several days before use.

Nuclear magnetic resonance spectra were measured on a JEOL ECA 500 spectrometer at 500 MHz for ^1H and 125 MHz for ^{13}C NMR. Melting points were measured with a capillary melting point apparatus and are not corrected. Electronic absorption spectra were recorded with a VARIAN Cary-50 UV–Vis spectrophotometer and were corrected for the background spectrum of the solvent. Emission spectra were obtained on a Perkin Elmer LS-50B luminescence spectrometer equipped with a Hamamatsu R928HA photomultiplier tube. Mass spectra were measured on Thermo LCQ deca XP ESI-MS. Elemental analyses were performed by NuMega Resonance Labs, San Diego, CA 92121. Electrochemical measurements were carried out using a BAS Epsilon electroanalytical system. Cyclic voltammetry experiments were performed at room temperature in one-compartment cell equipped with a glassy carbon working electrode, Ag/AgCl reference electrode and a Pt wire as the auxiliary electrode in acetonitrile containing tetrabutylammonium hexafluorophosphate (0.1 M) or in a pH 7 aqueous buffer (0.1 M NaTFA and 0.01 M phosphate) at a scan rate of 100 mV s^{-1} . The optimization of the structures of the dyads and the estimation of the Ru–Ru distances were carried out using Avogadro, an open source molecular builder and visualization tool, version 1.1.1.

4.2. Synthetic procedures

4.2.1. Ligand **4**

To a mixture of **14** (345 mg, 1 mmol), **15** (260 mg, 1 mmol), Pd (PPh_3) $_2\text{Cl}_2$ (35 mg, 5 mol%) and anhyd. K_2CO_3 (553 mg, 4 mmol) was added dry DMSO (5 mL) and degassed with N_2 for 15 min. The mixture was then heated at 100 °C for 24 h. After cooling, H_2O (10 mL) was added to the reaction mixture and the precipitate which formed was collected and washed with H_2O (20 mL), EtOH (20 mL), acetone (5 mL) and allowed to dry under vacuum to

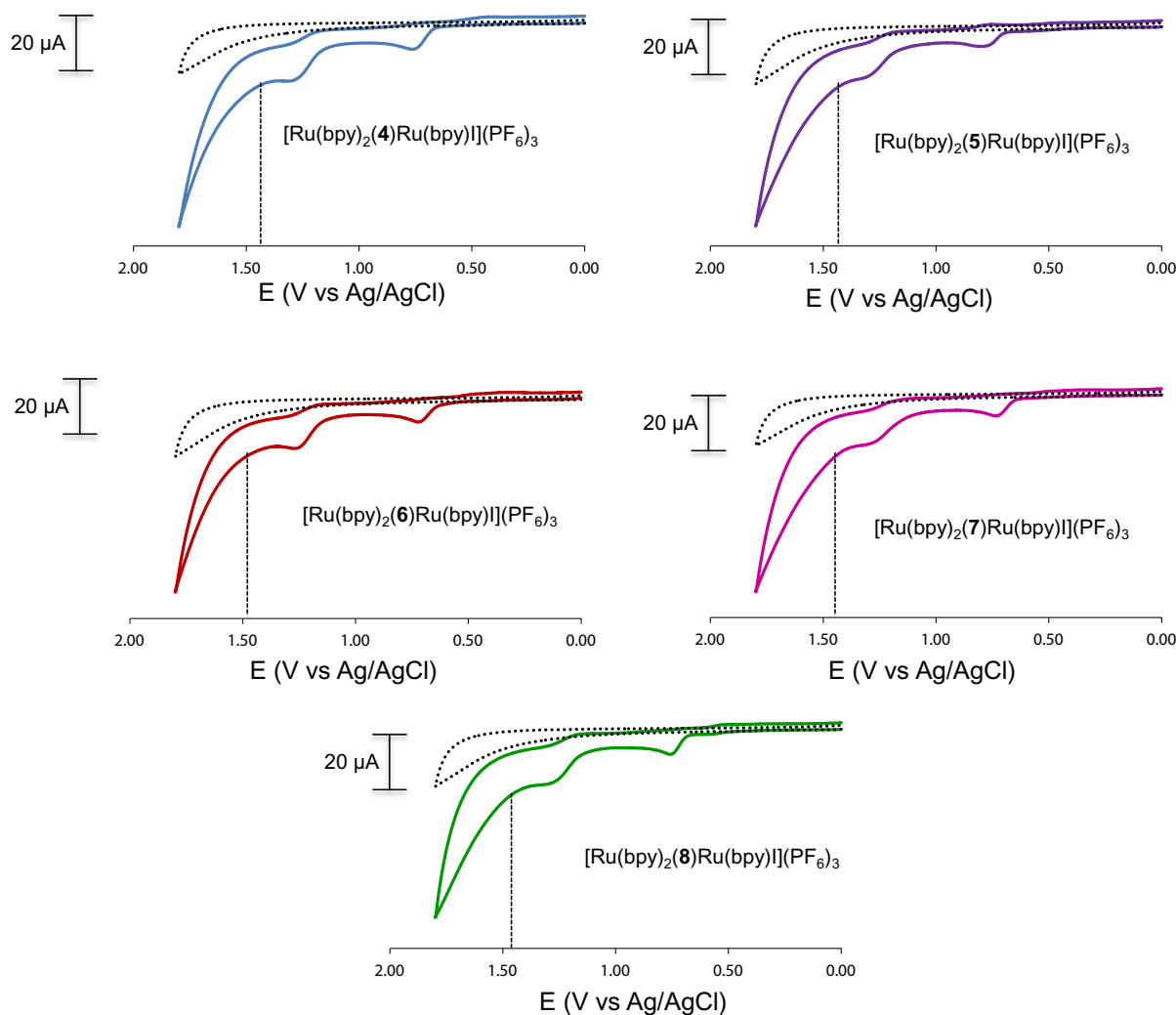


Fig. 13. Cyclic voltammograms of the dyads at pH 7 (0.1 M NaTFA and 0.01 M phosphate buffer). Conditions: glassy carbon working electrode, Ag/AgCl reference electrode, and Pt auxiliary electrode. Scan rate: 100 mV/s.

provide **4** as a brown solid (300 mg, 73%): mp 195 °C dec; ^1H NMR (500 MHz, CDCl_3) δ 9.32 (m, 2H), 8.77 (d, 2H, $J = 8.2$ Hz), 8.72 (m, 4H), 8.44 (d, 1H, $J = 8.2$ Hz), 8.39 (d, 1H, $J = 7.8$ Hz), 8.03 (s, 1H), 7.97 (t, 2H, $J = 7.5$ Hz), 7.76 (dd, 1H, $J = 7.8, 3.2$ Hz), 7.69 (dd, 1H, $J = 8.2, 4.1$ Hz), 7.42 (m, 2H); ^{13}C NMR (125 MHz, CDCl_3) δ 155.9, 155.8, 150.8, 150.4, 149.3, 148.9, 146.3, 146.1, 137.2, 136.8, 136.4, 134.3, 128, 127.2, 127.1, 124.2, 123.7, 123.3, 122.1, 121.6.

4.2.1.1. $[\text{Ru}(\text{bpy})_2(4)](\text{PF}_6)_2$. To a solution of **4** (50 mg, 0.12 mmol) in EtOH/ H_2O (3:1, 40 mL) at reflux was added a solution of $[\text{Ru}(\text{bpy})_2\text{Cl}_2]$ (62 mg, 0.012 mmol) in EtOH (10 mL) dropwise over 3 h, after which the reaction mixture was stirred at reflux for an additional 2 h. After cooling, the solution was concentrated under reduced pressure and treated with aq. NH_4PF_6 to provide an orange precipitate, which was collected and dried under vacuum. The crude solid was purified by column chromatography on alumina, eluting with $\text{CH}_2\text{Cl}_2/\text{acetone}$ (1:1) to afford the product as an orange solid (35 mg, 26%): ^1H NMR (400 MHz, acetone- d_6) δ 8.92 (d, 1H, $J = 8.2$ Hz), 8.84 (m, 6H), 8.72 (m, 5H), 8.59 (s, 1H), 8.52 (d, 2H, $J = 5.0$ Hz), 8.24 (m, 2H), 8.17 (m, 4H), 8.03 (m, 4H), 7.93 (m, 2H), 7.63 (m, 2H), 7.51 (m, 2H), 7.40 (m, 2H).

4.2.1.2. $[\text{Ru}(\text{bpy})_2(4)\text{Ru}(\text{bpy})\text{Cl}](\text{PF}_6)_3$. A solution of $[\text{Ru}(\text{bpy})_2(4)](\text{PF}_6)_2$ (35 mg, 0.03 mmol) and $[\text{Ru}(\text{bpy})(\text{dmsO})_2\text{Cl}_2]$ (15 mg,

0.03 mmol) was allowed to reflux for 14 h under N_2 . After cooling, the solvent was removed under reduced pressure, the residue was dissolved in H_2O and treated with NH_4PF_6 to provide a brown precipitate, which was collected and dried under vacuum. The solid was then purified by column chromatography on alumina, eluting with MeOH/acetone (4:100) to provide $[\text{Ru}(\text{bpy})_2(4)\text{Ru}(\text{bpy})\text{Cl}](\text{PF}_6)_3$ as a maroon solid (18 mg, 39%), which showed some impurities in the high field region (0–3 ppm) and was used in the next step without further purification: ^1H NMR (400 MHz, acetone- d_6) δ 10.36 (d, 1H, $J = 5.5$ Hz), 9.09 (d, 1H, $J = 8.7$ Hz), 9.06 (s, 2H), 8.85 (m, 8H), 8.70 (d, 2H, $J = 8.2$ Hz), 8.60 (d, 1H, $J = 8.2$ Hz), 8.54 (d, 2H, $J = 5.5$ Hz), 8.40 (m, 1H), 8.26 (m, 2H), 8.17 (m, 4H), 8.09 (m, 1H), 7.99 (m, 5H), 7.91 (d, 1H, $J = 5.5$ Hz), 7.87 (d, 2H, 5.0 Hz), 7.81 (t, 1H, $J = 7.8$ Hz), 7.70 (d, 1H, $J = 5.5$ Hz), 7.64 (t, 2H, $J = 6.4$ Hz), 7.46 (m, 4H), 7.10 (m, 1H).

4.2.1.3. $[\text{Ru}(\text{bpy})_2(4)\text{Ru}(\text{bpy})\text{I}](\text{PF}_6)_3$. A solution of $[\text{Ru}(\text{bpy})_2(4)\text{Ru}(\text{bpy})\text{Cl}](\text{PF}_6)_3$ (18 mg, 0.01 mmol) in acetone/ H_2O (1:1, 50 mL) was treated with KI (50 mg, 0.301 mmol) and allowed to stir at reflux for 2 days. The cooled reaction mixture was concentrated and treated with aq. NH_4PF_6 to provide a brown precipitate which was collected, washed with water and dried to afford $[\text{Ru}(\text{bpy})_2(4)\text{Ru}(\text{bpy})\text{I}](\text{PF}_6)_3$ (16 mg, 97%): ^1H NMR (400 MHz, acetone- d_6) δ 10.79 (d, 1H, $J = 5.9$ Hz), 9.11 (s, 2H), 9.06 (d, 1H, $J = 8.2$ Hz), 8.88

(m, 7H), 8.73 (d, 2H, $J = 7.8$ Hz), 8.61 (d, 2H, $J = 7.8$ Hz), 8.55 (m, 2H), 8.40 (m, 1H), 8.23 (m, 6H), 8.02 (m, 8H), 7.88 (m, 2H), 7.88 (m, 1H), 7.65 (m, 2H), 7.58 (d, 1H, $J = 5.5$ Hz), 7.45 (m, 4H), 7.16 (m, 1H). *Anal. Calc* for $C_{57}H_{41}F_{18}N_{11}P_3Ru_2$: C, 41.64; H, 2.51 N, 9.37. *Found*: C, 41.78 H, 2.90; N, 8.98%. *MS* (ESI): m/z 1499.97 $(M-PF_6)^+$, 677.49 $(M-2PF_6)^{2+}$, 403.35 $(M-3PF_6)^{3+}$.

4.2.2. Ligand 5

A mixture of **13** (315 mg, 1.01 mmol), **16** (205 mg, 1.01 mmol) and $Pd(PPh_3)_4$ (96 mg, 8 mol%) in a pressure tube was suspended in *n*-propylamine (10 mL) and degassed with N_2 for 15 min. The tube was sealed and heated at 80 °C for 24 h. By this time a brown precipitate had formed, which was collected and washed with water (20 mL), EtOH (20 mL) and Et_2O (5 mL) before drying under vacuum to provide **5** as a brown solid (230 mg, 81%): mp 202–208 °C; 1H NMR (500 MHz, $CDCl_3$) δ 9.32 (d, 1H, $J = 3.4$ Hz), 9.27 (d, 1H, $J = 2.3$ Hz), 8.99 (d, 1H, $J = 7.4$ Hz), 8.80 (m, 4H), 8.72 (d, 1H, $J = 8.0$ Hz), 8.33 (d, 1H, $J = 8.6$ Hz), 8.22 (s, 2H), 7.98 (m, 2H), 7.86 (m, 1H), 7.73 (dd, 1H, $J = 8.0, 4.6$ Hz), 7.45 (m, 2H); ^{13}C NMR (125 MHz, $DMSO-d_6$) δ 156.1, 154.7, 151.9, 151.3, 150.0, 146.3, 145.8, 138.2, 137.1, 134.9, 133.6, 132.6, 128.3, 127.9, 125.5, 124.7, 124.5, 122.7, 121.5, 118.2, 93.0, 90.8.

4.2.2.1. $[Ru(bpy)_2(5)](PF_6)_2$. Following the same procedure as $[Ru(bpy)_2(4)](PF_6)_2$, **5** (100 mg, 0.23 mmol) was treated with $[Ru(bpy)_2Cl_2]$ (119 mg, 0.23 mmol) to afford $[Ru(bpy)_2(5)](PF_6)_3$ as an orange solid (96 mg, 37%): 1H NMR (400 MHz, acetone- d_6) δ 9.31 (d, 1H, $J = 8.24$ Hz), 8.92 (s, 1H), 8.84 (m, 5H), 8.75 (m, 6H), 8.55 (d, 1H, $J = 5.5$ Hz), 8.51 (d, 1H, $J = 5.5$ Hz), 8.26 (m, 2H), 8.16 (m, 4H), 8.06 (m, 3H), 7.96 (m, 3H), 7.64 (m, 2H), 7.52 (m, 2H), 7.40 (m, 2H).

4.2.2.2. $[Ru(bpy)_2(5)Ru(bpy)Cl](PF_6)_3$. Following the same procedure as $[Ru(bpy)_2(4)Ru(bpy)Cl](PF_6)_2$, $[Ru(bpy)_2(5)](PF_6)_2$ (38 mg, 0.03 mmol) and $[Ru(bpy)(dmsO)_2Cl_2]$ (16 mg, 0.03 mmol) were reacted to provide a crude solid which was then purified twice by column chromatography on alumina, eluting with MeOH/acetone (4:100) to provide $[Ru(bpy)_2(5)Ru(bpy)Cl](PF_6)_3$ as a maroon solid (7 mg, 15%): 1H NMR (400 MHz, acetone- d_6) δ 10.38 (d, 1H, $J = 5.0$ Hz), 9.80 (d, 1H, $J = 8.7$ Hz), 9.53 (s, 1H), 9.31 (s, 1H), 8.87 (m, 9H), 8.59 (d, 1H, $J = 8.2$ Hz), 8.44 (m, 3H), 8.26 (m, 2H), 8.25 (m, 2H), 8.14 (m, 7H), 8.01 (d, 1H, $J = 5.5$ Hz), 7.92 (dd, 1H, $J = 8.2, 4.1$ Hz), 7.80 (m, 4H), 7.64 (m, 2H), 7.58 (d, 1H, $J = 5.0$ Hz), 7.49 (t, 1H, $J = 6.4$ Hz), 7.42 (m, 1H), 7.36 (m, 1H), 7.06 (m, 2H).

4.2.2.3. $[Ru(bpy)_2(5)Ru(bpy)I](PF_6)_3$. Following the same procedure as $[Ru(bpy)_2(4)Ru(bpy)I](PF_6)_3$, $[Ru(bpy)_2(5)Ru(bpy)Cl](PF_6)_3$ (7 mg, 0.004 mmol) was treated with KI (50 mg, 0.301 mmol) to afford $[Ru(bpy)_2(5)Ru(bpy)I](PF_6)_3$ (5 mg, 75%): 1H NMR (400 MHz, acetone- d_6) δ 10.75 (d, 1H, $J = 5.7$ Hz), 9.35 (d, 1H, $J = 8.0$ Hz), 9.06 (s, 2H), 8.86 (m, 8H), 8.71 (m, 2H), 8.59 (d, 1H, $J = 8.0$ Hz), 8.53 (d, 1H, $J = 5.1$ Hz), 8.51 (d, 1H, $J = 5.7$ Hz), 8.26 (m, 2H), 8.16 (m, 4H), 8.05 (m, 2H), 7.98 (m, 7H), 7.87 (m, 1H), 7.64 (m, 2H), 7.52 (d, 1H, $J = 5.7$ Hz), 7.42 (m, 4H), 7.16 (m, 1H). *Anal. Calcd* for $C_{59}H_{41}F_{18}N_{11}P_3Ru_2$: C, 42.48; H, 2.48; N, 9.24. *Found*: C, 42.86 H, 2.87 N, 8.96%. *MS* (ESI): m/z 1522.97 $(M-PF_6)^+$, 689.47 $(M-2PF_6)^{2+}$, 411.02 $(M-3PF_6)^{3+}$.

4.2.3. Ligand 6

To a mixture of **18** (274 mg, 0.63 mmol), **15** (163 mg, 0.63 mmol), $Pd(PPh_3)Cl_2$ (22 mg, 5 mol%) and anhyd. K_2CO_3 (261 mg, 1.89 mmol) was added dry DMSO (5 mL) and degassed for 15 min. The mixture was then heated at 100 °C for 24 h. After cooling, H_2O (10 mL) was added to the reaction mixture and the precipitate that had formed was collected and washed with H_2O (20 mL), EtOH (20 mL), acetone (5 mL) and allowed to dry under

vacuum to provide **6** as a tan-colored solid (240 mg, 70%): mp 220 °C dec; 1H NMR (500 MHz, $CDCl_3$) δ 9.23 (m, 2H), 8.85 (s, 2H), 8.75 (d, 2H, $J = 4.01$ Hz), 8.71 (d, 2H, $J = 9.16$ Hz), 8.32 (m, 2H), 8.10 (d, 2H, $J = 8.02$ Hz), 7.91 (dt, 2H, $J = 8.02, 1.72$ Hz), 7.83 (s, 1H), 7.69 (m, 3H), 7.63 (m, 1H), 7.38 (m, 2H); ^{13}C NMR (125 MHz, $DMSO-d_6$) δ 156.4, 155.4, 150.8, 150.4, 149.9, 149.5, 146.4, 145.7, 140.1, 138.1, 137.9, 137.6, 136.9, 134.6, 131.5, 128.4, 127.8, 127.6, 127.5, 125.2, 124.3, 123.9, 121.5, 118.5.

4.2.3.1. $[Ru(bpy)_2(6)](PF_6)_2$. Following the same procedure as $[Ru(bpy)_2(4)](PF_6)_2$, **6** (100 mg, 0.205 mmol) was treated with $[Ru(bpy)_2Cl_2]$ (107 mg, 0.205 mmol) to afford $[Ru(bpy)_2(6)](PF_6)_2$ as an orange solid (61 mg, 25%): 1H NMR (400 MHz, acetone- d_6) δ 8.83 (d, 2H, $J = 5.7$ Hz), 8.71 (m, 4H), 8.61 (d, 1H, $J = 8.2$ Hz), 8.50 (m, 5H), 8.25 (d, 1H, $J = 8.5, 3.2$ Hz), 8.09 (m, 6H), 7.98 (m, 4H), 7.84 (d, 2H, $J = 5.5$ Hz), 7.77 (m, 3H), 7.68 (m, 1H), 7.58 (m, 2H), 7.43 (m, 4H), 7.24 (m, 2H).

4.2.3.2. $[Ru(bpy)_2(6)Ru(bpy)Cl](PF_6)_3$. Following the same procedure as $[Ru(bpy)_2(4)Ru(bpy)Cl](PF_6)_2$, $[Ru(bpy)_2(6)](PF_6)_2$ (55 mg, 0.046 mmol) was treated with $[Ru(bpy)(dmsO)_2Cl_2]$ (22 mg, 0.045 mmol) to provide $[Ru(bpy)_2(6)Ru(bpy)Cl](PF_6)_3$ as a maroon solid (10 mg, 13%): 1H NMR (500 MHz, acetone- d_6) δ 10.34 (d, 1H, $J = 4.6$ Hz), 9.19 (s, 2H), 8.84 (m, 9H), 8.70 (d, 1H, $J = 8.6$ Hz), 8.59 (d, 1H, $J = 8.6$ Hz), 8.53 (d, 1H, $J = 8.6$ Hz), 8.49 (m, 3H), 8.37 (m, 1H), 8.25 (m, 2H), 8.16 (m, 4H), 8.08 (m, 1H), 7.98 (m, 9H), 7.84 (d, 1H, $J = 5.1$ Hz), 7.81 (m, 1H), 7.65 (m, 3H), 7.42 (m, 4H), 7.10 (m, 1H).

4.2.3.3. $[Ru(bpy)_2(6)Ru(bpy)I](PF_6)_3$. Following the same procedure as $[Ru(bpy)_2(4)Ru(bpy)I](PF_6)_2$, $[Ru(bpy)_2(6)Ru(bpy)Cl](PF_6)_3$ (10 mg, 0.006 mmol) was treated with KI (50 mg, 0.301 mmol) to afford $[Ru(bpy)_2(6)Ru(bpy)I](PF_6)_3$ (8 mg, 82%): 1H NMR (500 MHz, acetone- d_6) δ 10.78 (d, 1H, $J = 5.0$ Hz), 9.24 (s, 2H), 8.86 (m, 8H), 8.71 (d, 1H, $J = 7.3$ Hz), 8.57 (m, 3H), 8.51 (m, 3H), 8.39 (m, 1H), 8.27 (m, 2H), 8.18 (m, 4H), 7.98 (m, 11H), 7.88 (m, 1H), 7.65 (m, 2H), 7.54 (d, 1H, $J = 5.0$ Hz), 7.44 (m, 4H), 7.17 (m, 1H). *Anal. Calc.* for $C_{63}H_{45}F_{18}N_{11}P_3Ru_2$: C, 43.99; H, 2.64; N, 8.96. *Found*: C, 44.05; H, 3.00; N, 8.65%. *MS* (ESI): m/z 1575.99 $(M-PF_6)^+$, 715.46 $(M-2PF_6)^{2+}$, 428.75 $(M-3PF_6)^{3+}$.

4.2.4. Ligand 7

To a mixture of **16** (205 mg, 1 mmol), **17** (323.5 mg, 0.83 mmol) and $Pd(PPh_3)_4$ (96 mg, 8 mol%) in a pressure tube was added *n*-propylamine (20 mL) and the mixture was degassed with N_2 for 15 min. The tube was then sealed and heated at 80 °C for 40 h. The reaction mixture was cooled and the precipitate which had formed was filtered, washed with water (20 mL), EtOH (20 mL) and diethyl ether (10 mL) and dried under vacuum to afford **7** as a tan solid (280 mg, 66%): mp >260 °C; 1H NMR (500 MHz, $CDCl_3$) δ 9.26 (d, 1H, $J = 4.1$ Hz), 9.21 (d, 1H, $J = 4.1$ Hz), 8.88 (d, 1H, $J = 8.2$ Hz), 8.80 (s, 2H), 8.76 (d, 2H, $J = 4.1$ Hz), 8.70 (d, 2H, $J = 7.8$ Hz), 8.26 (d, 1H, $J = 7.5$ Hz), 8.15 (s, 1H), 8.0 (d, 2H, $J = 7.3$ Hz), 7.91 (t, 2H, $J = 7.3$ Hz), 7.80 (m, 3H), 7.39 (m, 2H); ^{13}C NMR (125 MHz, $CDCl_3$) δ 156.2, 151.1, 150.8, 149.3, 146.3, 146.1, 139.0, 137.1, 135.9, 134.9, 132.4, 130.9, 128.4, 128.2, 127.6, 124.1, 123.6, 123.4, 121.5, 119.9, 118.8, 95.2, 87.3.

4.2.4.1. $[Ru(bpy)_2(7)](PF_6)_2$. Following the same procedure as $[Ru(bpy)_2(4)](PF_6)_2$, **7** (100 mg, 0.195 mmol) was treated with $[Ru(bpy)_2Cl_2]$ (101 mg, 0.195 mmol) to afford $[Ru(bpy)_2(7)](PF_6)_2$ as an orange solid (101 mg, 43%): 1H NMR (500 MHz, acetone- d_6) δ 9.21 (d, 1H, $J = 8.2$ Hz), 8.83 (m, 7H), 8.74 (m, 5H), 8.51 (d, 1H, $J = 5.0$ Hz), 8.46 (d, 1H, $J = 5.5$ Hz), 8.24 (m, 2H), 8.15 (m, 4H), 8.10 (m, 3H), 8.01 (m, 5H), 7.94 (m, 3H), 7.62 (m, 2H), 7.48 (m, 2H), 7.38 (m, 2H).

4.2.4.2. $[Ru(bpy)_2(7)Ru(bpy)Cl](PF_6)_3$. Following the same procedure as $[Ru(bpy)_2(4)Ru(bpy)Cl](PF_6)_2$, $[Ru(bpy)_2(7)](PF_6)_2$ (50 mg, 0.041 mmol) was reacted with $[Ru(bpy)(dmsO)_2Cl_2]$ (20 mg, 0.041 mmol) to provide $[Ru(bpy)_2(7)Ru(bpy)Cl](PF_6)_3$ as a maroon solid (28 mg, 41%): 1H NMR (500 MHz, acetone- d_6) δ 10.33 (d, 1H, $J = 5.7$ Hz), 9.22 (d, 1H, $J = 5.7$ Hz), 9.14 (s, 1H), 8.85 (m, 8H), 8.74 (s, 1H), 8.60 (d, 1H, $J = 8.0$ Hz), 8.53 (d, 1H, $J = 4.6$ Hz), 8.47 (d, 1H, $J = 5.1$ Hz), 8.39 (m, 3H), 8.25 (m, 2H), 8.16 (m, 3H), 8.01 (m, 5H), 7.95 (m, 3H), 7.84 (d, 1H, 5.1 Hz), 7.80 (m, 1H), 7.63 (m, 3H), 7.40 (m, 4H), 7.10 (m, 1H).

4.2.4.3. $[Ru(bpy)_2(7)Ru(bpy)I](PF_6)_3$. Following the same procedure as $[Ru(bpy)_2(4)Ru(bpy)I](PF_6)_2$, $[Ru(bpy)_2(7)Ru(bpy)Cl](PF_6)_3$ (28 mg, 0.017 mmol) was treated with KI (50 mg, 0.301 mmol) to afford $[Ru(bpy)_2(7)Ru(bpy)I](PF_6)_3$ (24 mg, 82%): 1H NMR (500 MHz, acetone- d_6) δ 10.77 (d, 1H, $J = 5.0$ Hz), 9.23 (m, 1H), 9.19 (s, 2H), 8.85 (m, 8H), 8.75 (s, 1H), 8.60 (d, 1H, $J = 8.0$ Hz), 8.53 (dd, 1H, $J = 5.7, 1.4$ Hz), 8.46 (m, 3H), 8.38 (m, 1H), 8.25 (m, 2H), 8.15 (m, 4H), 8.21 (m, 11H), 7.87 (m, 1H), 7.63 (m, 2H), 7.54 (d, 1H, 5.15 Hz), 7.41 (m, 4H), 7.16 (m, 1H). *Anal. Calc.* for $C_{65}H_{45}F_{18}N_{11}P_3Ru_2$: C, 44.76; H, 2.60; N, 8.83. *Found*: C, 45.11; H, 2.98; N, 8.43%. *MS (ESI)*: m/z 1599.00 (M– PF_6) $^+$, 727.00 (M– $2PF_6$) $^{2+}$, 436.68 (M– $3PF_6$) $^{3+}$.

4.2.5. Compound 20

To a mixture of **16** (205 mg, 1 mmol), **19** (510 mg, 2 mmol) and $Pd(PPh_3)_4$ (58 mg, 5 mol%) in a pressure tube, *n*-propylamine (15 mL) was added and degassed with N_2 for 15 min. The tube was then sealed and heated at 80 °C for 18 h. After cooling, the solvent was removed under reduced pressure and the residue was purified by column chromatography on silica gel, eluting with MeOH– CH_2Cl_2 (2:98) to provide the TMS-protected coupling product which was then deprotected by stirring overnight in a suspension of K_2CO_3 in MeOH at rt. After removing the solvent under reduced pressure, the residue was purified by column chromatography on silica gel, eluting with MeOH– CH_2Cl_2 (2:98) to provide **20** as a yellow solid (248 mg, 82%): mp 180 °C dec; 1H NMR (500 MHz, $CDCl_3$) δ 9.23 (dd, 1H, $J = 4.6, 1.7$ Hz), 9.19 (dd, 1H, $J = 4.6, 1.7$ Hz), 8.80 (dd, 1H, $J = 8.0, 1.7$ Hz), 8.24 (dd, 1H, $J = 8.0, 1.7$ Hz), 8.10 (s, 1H), 7.74 (dd, 1H, $J = 8.6, 4.6$ Hz), 7.66 (dd, 1H, $J = 8.6, 4.6$ Hz), 7.62 (d, 2H, $J = 8.6$ Hz), 7.54 (d, 2H, $J = 8.6$ Hz), 3.22 (s, 1H).

4.2.6. Ligand 8

A mixture of **13** (165 mg, 0.53 mmol), **19** (161 mg, 0.53 mmol) and $Pd(PPh_3)_4$ (31 mg, 5 mol%) in a pressure tube was suspended in *n*-propylamine (10 mL) and degassed with N_2 for 15 min. The tube was sealed and heated at 80 °C for 18 h. By this time a brown precipitate had formed, which was collected and washed with EtOH (20 mL) and Et_2O (5 mL) before drying under vacuum to provide **8** as a yellow solid (230 mg, 81%): mp 244–248 °C; 1H NMR (500 MHz, $CDCl_3$) δ 9.25 (d, 1H, $J = 4.0$ Hz), 9.21 (d, 1H, $J = 4.6$ Hz), 8.83 (d, 1H, $J = 8.0$ Hz), 8.73 (d, 2H, $J = 4.6$ Hz), 8.61 (m, 3H), 8.26 (d, 1H, $J = 8.0$ Hz), 8.13 (s, 2H), 7.89 (m, 2H), 7.76 (m, 1H), 7.65 (m, 6H), 7.37 (m, 2H); ^{13}C NMR (125 MHz, $CDCl_3$) δ 155.7, 151.1, 150.8, 149.3, 146.3, 146.0, 137.1, 135.9, 134.8, 133.1, 132.2, 132.0, 131.9, 131.8, 131.8, 131.0, 128.3, 128.1, 124.2, 123.6, 123.5, 123.3, 123.1, 122.8, 121.3, 119.7, 95.0, 93.2, 89.8, 88.1.

4.2.6.1. $[Ru(bpy)_2(8)](PF_6)_2$. Following the same procedure as $[Ru(bpy)_2(4)](PF_6)_2$, **8** (96 mg, 0.18 mmol) was treated with $[Ru(bpy)_2Cl_2]$ (93 mg, 0.18 mmol) to afford $[Ru(bpy)_2(8)](PF_6)_2$ as an orange solid (87 mg, 39%). 1H NMR (400 MHz, acetone- d_6) δ 9.17 (dd, 1H, $J = 8.0, 1.1$ Hz), 8.84 (m, 2H), 8.79 (m, 3H), 8.72 (m, 3H), 8.70 (s, 2H), 8.60 (s, 2H), 8.50 (dd, 1H, $J = 5.1, 1.1$ Hz), 8.46 (dd, 1H, $J = 5.1, 1.1$ Hz), 8.24 (m, 2H), 8.14 (m, 4H), 8.01 (m, 3H), 7.93

(m, 3H), 7.86 (dd, 4H, $J = 17.7, 8.6$ Hz), 7.62 (m, 2H), 7.49 (m, 2H), 7.38 (m, 2H).

4.2.6.2. $[Ru(bpy)_2(8)Ru(bpy)Cl](PF_6)_3$. Following the same procedure as $[Ru(bpy)_2(4)Ru(bpy)Cl](PF_6)_2$, $[Ru(bpy)_2(8)](PF_6)_2$ (53 mg, 0.04 mmol) was treated with $[Ru(bpy)(dmsO)_2Cl_2]$ (21 mg, 0.04 mmol) to provide $[Ru(bpy)_2(8)Ru(bpy)Cl](PF_6)_3$ as a maroon solid (20 mg, 28%): 1H NMR (500 MHz, acetone- d_6) δ 10.36 (d, 1H, $J = 5.5$ Hz), 9.19 (dd, 1H, $J = 8.2, 1.4$ Hz), 8.85 (m, 5H), 8.80 (d, 1H, $J = 8.2$ Hz), 8.71 (s, 1H), 8.60 (m, 3H), 8.51 (dd, 1H, $J = 5.5, 1.4$ Hz), 8.46 (dd, 1H, $J = 5.5, 1.4$ Hz), 8.41 (td, 1H, $J = 7.8, 1.4$ Hz), 8.24 (m, 2H), 8.14 (m, 5H), 8.03 (dd, 1H, $J = 8.2, 5.0$ Hz), 7.89 (m, 9H), 7.79 (m, 3H), 7.63 (m, 2H), 7.55 (d, 1H, $J = 5.9$ Hz), 7.38 (m, 4H), 7.08 (m, 1H).

4.2.6.3. $[Ru(bpy)_2(8)Ru(bpy)I](PF_6)_3$. Following the same procedure as $[Ru(bpy)_2(4)Ru(bpy)I](PF_6)_2$, $[Ru(bpy)_2(8)Ru(bpy)Cl](PF_6)_3$ (10 mg, 0.006 mmol) was treated with KI (50 mg, 0.301 mmol) to afford $[Ru(bpy)_2(8)Ru(bpy)I](PF_6)_3$ (8 mg, 76%): 1H NMR (500 MHz, acetone- d_6) δ 10.77 (d, 1H, $J = 5.0$ Hz), 9.23 (m, 1H), 9.19 (s, 2H), 8.85 (m, 8H), 8.75 (s, 1H), 8.60 (d, 1H, $J = 8.0$ Hz), 8.53 (dd, 1H, $J = 5.7, 1.4$ Hz), 8.46 (m, 3H), 8.38 (m, 1H), 8.25 (m, 2H), 8.15 (m, 4H), 8.01 (m, 11H), 7.87 (m, 1H), 7.63 (m, 2H), 7.54 (d, 1H, $J = 5.2$ Hz), 7.41 (m, 4H), 7.16 (m, 1H). ^{13}C NMR (150 MHz, CD_3CN) δ 158.24, 158.05, 157.30, 157.22, 157.03, 155.80, 153.22, 152.99, 152.12, 152.08, 151.02, 147.76, 147.55, 137.99, 137.87, 137.22, 136.69, 136.66, 136.40, 135.43, 132.49, 132.36, 132.06, 132.02, 130.73, 130.58, 127.64, 127.51, 127.13, 126.62, 126.34, 124.36, 124.34, 124.29, 124.25, 124.10, 123.87, 123.80, 122.99, 122.95, 121.35, 96.65, 94.77, 89.04, 86.51. *MS (ESI)*: m/z 1622.81 (M– PF_6) $^+$, 739.45 (M– $2PF_6$) $^{2+}$, 444.69 (M– $3PF_6$) $^{3+}$.

Acknowledgements

We gratefully acknowledge financial support of this work by the Robert A. Welch Foundation through Grant E-621. We also thank Dr. Marten Ahlquist at the KTH Royal Institute of Technology in Sweden for assistance with DFT calculations and Dr. Husain Kagalwala for assistance with the electron transfer distance measurements.

Appendix A. Supplementary material

Supplementary data associated with this article can be found, in the online version, at <http://dx.doi.org/10.1016/j.ica.2016.02.057>.

References

- [1] J.J. Concepcion, J.W. Jurss, M.K. Brennaman, P.G. Hoertz, A.O.T. Patrocinio, N.Y. M. Iha, J.L. Templeton, T.J. Meyer, *Acc. Chem. Res.* 42 (2009) 1954.
- [2] N. Kaveevivitchai, R. Chitta, R. Zong, M. El Ojaimi, R.P. Thummel, *J. Am. Chem. Soc.* 134 (2012) 10721.
- [3] D.L. Ashford, D.J. Stewart, C.R. Glasson, R.A. Binstead, D.P. Harrison, M.R. Norris, J.J. Concepcion, Z. Fang, J.L. Templeton, *Inorg. Chem.* 51 (2012) 6428.
- [4] F. Li, Y. Jiang, B. Zhang, F. Huang, Y. Gao, L. Sun, *Angew. Chem. Int. Ed.* 51 (2012) 2417.
- [5] M. Hissler, W.B. Connick, D.K. Geiger, J.E. McGarrah, D. Lipa, R.J. Lachicotte, R. Eisenberg, *Inorg. Chem.* 39 (2000) 447.
- [6] R. Ziessel, J. Suffert, M.-T. Youinou, *J. Org. Chem.* 61 (1996) 6535.
- [7] J. Wang, G.S. Hanan, *Synlett* 8 (2005) 1251.
- [8] J.P. Sauvage, J.P. Collin, J.C. Chambron, S. Guillerez, C. Coudret, V. Balzani, F. Barigelli, L. Decola, L. Flamigni, *Chem. Rev.* 94 (1994) 993.
- [9] E.C. Constable, M.D. Ward, *J. Chem. Soc., Dalton Trans.* (1990) 1405.
- [10] K.T. Potts, D. Konwar, *J. Org. Chem.* 56 (1991) 4815.
- [11] S. Katagiri, R. Sakamoto, H. Maeda, Y. Nishimori, T. Kurita, H. Nishihara, *Chem. Eur. J.* 19 (2013) 5088.
- [12] C.J. Aspley, J.A.G. Williams, *New J. Chem.* 25 (2001) 1136.
- [13] M. Toyama, K. Inoue, S. Iwamatsu, N. Nagao, *Bull. Chem. Soc. Jpn.* 79 (2006) 1525.
- [14] B.P. Sullivan, D.J. Salmon, T.J. Meyer, *Inorg. Chem.* 17 (1978) 334.
- [15] M.D. Hossain, M. Higuchi, *Synthesis* 45 (2013) 753.
- [16] V. Grosshenny, R. Ziessel, *J. Organomet. Chem.* 453 (1993) C19.